

Konya Mühendislik Bilimleri Dergisi, c. 13, s. 3, 880-891, 2025 Konya Journal of Engineering Sciences, v. 13, n. 3, 880-891, 2025 ISSN: 2667-8055 (Electronic)

DOI: 10.36306/konjes.1678776

TAILORING IONIC CONDUCTIVITY OF CHITOSAN FILMS THROUGH CONTROLLED LACTIC ACID INCORPORATION

^{1,*} Doga DOGANAY ©

¹ Middle East Technical University (METU), Department of Metallurgical and Materials Engineering, Ankara, TÜRKİYE

¹doganay@metu.edu.tr

Highlights

- Lactic acid content significantly affects the crystallinity and thermal stability of chitosan films.
- A cost-effective solvent casting method is employed fabricate chitosan films.
- Ionic conductivity of chitosan films increase with increasing lactic acid content.

ISSN: 2667-8055 (Electronic) DOI: 10.36306/konjes.1678776



TAILORING IONIC CONDUCTIVITY OF CHITOSAN FILMS THROUGH CONTROLLED LACTIC ACID INCORPORATION

^{1,*} Doga DOGANAY

¹ Middle East Technical University (METU), Department of Metallurgical and Materials Engineering, Ankara, TÜRKİYE

¹doganay@metu.edu.tr

(Received: 17.04.2025; Accepted in Revised Form: 28.06.2025)

ABSTRACT: Chitosan, a biodegradable and biocompatible biopolymer, is widely utilized due to its excellent film-forming capability and versatile applicability in various industries, including food packaging, pharmaceuticals, agriculture, and bioelectronics. This study investigates the influence of lactic acid concentration (2 wt%, 4 wt%, and 6 wt%) on the structural, thermal, and electrochemical properties of chitosan films. Films were prepared by dissolving chitosan in lactic acid solutions and casting them via solvent casting. Structural properties were characterized using X-ray diffraction (XRD) and Fourier transform infrared spectroscopy (FTIR), thermal stability was analyzed by thermogravimetric analysis (TGA), and electrochemical properties were examined through ionic conductivity and capacitance measurements. The results reveal that increasing lactic acid concentration enhances ionic conductivity and areal capacitance of the chitosan films. At the highest lactic acid content (6 wt%), the films exhibited an ionic conductivity of 2.6×10^{-4} S/cm and an areal capacitance of 7.14 µF/cm² at 100 Hz. The results demonstrate the high potential of chitosan films for use in flexible energy storage systems, capacitive sensors and implantable bioelectronic devices.

Keywords: Chitosan Films, Lactic Acid, Ionic Conductivity

1. INTRODUCTION

Chitosan, a versatile biopolymer derived through the deacetylation of chitin, has attracted significant attention due to its outstanding biocompatibility, biodegradability, and antimicrobial properties. Chitin, primarily sourced from the exoskeletons of crustaceans, is the second most abundant natural polymer after cellulose [1]. The transformation of chitin into chitosan imparts unique and desirable properties such as bioadhesion, film-forming capability, and antibacterial activity, making it suitable for diverse applications across several industries, including pharmaceuticals, food packaging, water treatment, agriculture, textile, cosmetics, and biomedical engineering [2]. In the pharmaceutical industry, chitosan has been extensively utilized due to its compatibility with biological systems. Its unique ability to form hydrogels and nanoparticles facilitates controlled drug release, enhancing its effectiveness as a drug delivery system [3], [4]. Additionally, chitosan's natural antimicrobial properties and ability to stimulate wound healing processes have significantly advanced its use in therapeutic applications, such as wound dressings, sutures, and implant coatings [5]. These applications exploit chitosan's intrinsic capability to support cell adhesion, proliferation, and tissue regeneration. Within the food industry, chitosan-based materials have emerged as a promising solution for packaging and preservation due to their antimicrobial activity and barrier properties against oxygen and moisture [6], [7], [8]. These films help extend shelf life and maintain product quality, aligning with consumer preferences for natural, non-toxic, and biodegradable packaging materials. Additionally, chitosan films demonstrate substantial potential in agriculture, where they serve as bio-based coatings on seeds, enhancing germination rates, improving nutrient uptake, and providing protection against pests and pathogens [9].

In the field of electronics, chitosan has emerged as a promising material as active layers and substrates due to its inherent ionic conductivity, and the ability to form versatile thin films and

hydrogels [10], [11]. Chitosan-based bioelectronic devices can effectively interface with biological tissues, facilitating the transduction of biological signals into electronic signals [12]. Its proton-conducting ability and responsive properties to environmental stimuli such as pH, temperature, and humidity have led to its incorporation into sensors, actuators, and wearable electronic devices [13], [14], [15]. Furthermore, the biodegradability and biocompatibility of chitosan enable its use in implantable electronics, where it not only supports long-term biocompatibility but also minimizes adverse inflammatory responses [12]. The integration of chitosan into bioelectronic platforms thus represents an innovative step forward, opening avenues for advanced medical diagnostics, therapeutics, and personalized healthcare applications.

Chitosan is frequently processed into film form due to its advantageous for various applications requiring thin, flexible, and durable materials. Typically, these films are produced by dissolving chitosan in an acidic aqueous medium, a process that protonates the amino groups and enhances solubility, facilitating uniform film formation [16]. The type and concentration of acid significantly affect the resulting films' physicochemical characteristics. Acetic acid has conventionally been the solvent of choice due to its effectiveness in dissolving chitosan and producing mechanically robust films [17], [18]. However, its use in high concentrations poses considerable environmental concerns, such as corrosion of processing equipment and toxicity challenges, leading researchers to seek alternative acids [19], [20]. Lactic acid has emerged as a particularly promising alternative solvent due to its inherent plasticizing effects, which enable the production of films with enhanced flexibility and mechanical resilience films [21], [22], [23]. Its biodegradability and lower environmental impact further enhance its appeal for sustainable material production. Moreover, lactic acid's structural and chemical compatibility with chitosan allows the formation of homogeneous and structurally stable films that exhibit superior plasticity compared to those prepared with acetic acid [17]. While previous studies have extensively explored the influence of lactic acid concentration on the mechanical, thermal, and permeability properties of chitosan films, the electrochemical aspects remain relatively understudied. Electrochemical properties, such as ionic conductivity, dielectric constant, and capacitance, are crucial for the applicability of chitosan films in advanced technological domains, including energy storage devices, capacitive sensors, wearable electronics, biosensors, and implantable biomedical devices. Enhanced ionic conductivity and capacitance are particularly desirable for the development of flexible and efficient energy storage systems and sensors. Room-temperature ionic conductivities in the range of 10⁻⁵-10⁻⁴ S/cm are generally considered sufficient for flexible polymer gel electrolytes used in low-power devices such as wearable electronics, sensors, and thin-film systems [24], [25].

This study aims to systematically investigate the effects of varying lactic acid concentrations (2 wt%, and 6 wt%) on the structural, thermal, and specifically electrochemical properties of chitosan films. These films are produced using a solvent casting method, an economical and widely accepted technique. Characterization techniques, including X-ray diffraction (XRD), Fourier transform infrared spectroscopy (FTIR), and thermogravimetric analysis (TGA), are employed to evaluate the structural integrity and thermal stability of the films. Additionally, electrochemical analyses, encompassing ionic conductivity and capacitance measurements, provide detailed insights into the electrical performance of the films. This study investigates how different concentrations of lactic acid influence the electrochemical properties of chitosan films. By clarifying the relationship between structural, thermal, and electrochemical characteristics, the research provides practical insights for optimizing chitosan-based materials. These findings can directly support the development of improved electrochemical applications, including energy storage devices, capacitive sensors, wearable electronics, and implantable biomedical devices thus contributing to advancements in sustainable and eco-friendly material technologies.

2. MATERIAL AND METHODS

2.1. Materials

Chitosan powders (medium molecular weight, >75% deacetylated) and Lactic Acid (DL-Lactic Acid

90% (T)) were purchased from Sigma Alldrich. Deionized (DI) water with a resistivity of 18.2 Mohm.cm was used. Acetone (99.8%), ethanol (98.85%) was purchased Sigma-Aldrich.

2.2. Preparation of Chitosan Films

All glassware was sonicated in acetone, ethanol and DI water for 10 minutes, respectively, and dried in an oven at 100 °C before the experiment. Schematic representation of the preparation steps of chitosan films is provided in **Figure 1.** 400 mg of Chitosan powders were dissolved in 20 ml lactic acid DI water solution with different lactic acid concentrations (2 wt%, 4 wt% and 6 wt%). Mixtures were stirred at 40°C overnight. The solution was centrifuged at 7000 rpm for 10 minutes to separate insoluble chitosan powders. 15 grams of each solution were cast into glass petri dishes with a diameter of 4 cm. Excess water in the solution was removed by keeping the petri dishes in a vacuum oven at 40°C overnight. Then Chitosan films were carefully removed from the petri dishes for further characterizations.

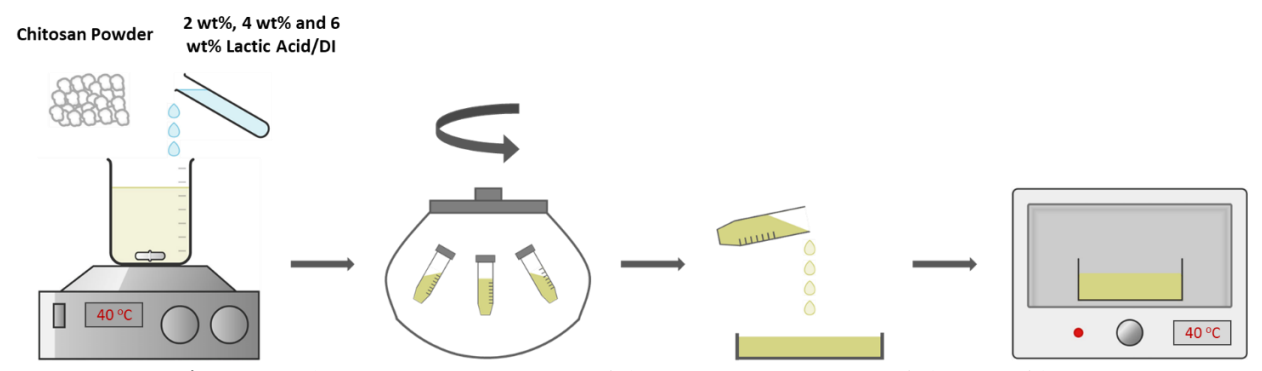


Figure 1: Schematic representation of the preparation stages of chitosan films.

2.3. Characterizations

Crystal structures of the chitosan films were investigated via XRD analysis were conducted via Bruker D8 Avance using Cu-K α radiation (0.153nm) operating between 0-40 $^{\circ}$ at a scanning speed of 0.2 $^{\circ}$ min⁻¹. The crystallinity index (CrI) of chitosan powder and chitosan films fabricated with different lactic acid concentrations was calculated using the Segal method [26]:

$$CrI\ (\%) = \frac{l_{(200)} - I_{am}}{I_{(200)}} \times 100$$

where $l_{(200)}$ is the maximum intensity of the (200) diffraction peak at 2θ =20.2° and l_{am} is the intensity of the amorphous region at 2θ =16°.

Fourier transform-infrared (FTIR) spectroscopy was caried out by attenuated total reflectance (ATR) unit of FTIR spectrometer (Shimadzu IRTracerTM_100) with a resolution of 4 cm⁻¹ within a wavenumber range of 400-4000 cm⁻¹. Thermal degradation characteristics of the chitosan films were investigated via thermogravimetric analysis (TGA). TGA was performed using Exstar SII TG/DTA 7300 system under nitrogen atmosphere with a temperature increment rate of 10 °C/min within the temperature range of 30-550 °C. In XRD analysis, FTIR spectroscopy, and TGA, chitosan powders were used as received without any further processing for comparison with chitosan films fabricated with different lactic acid concentration.

Electrochemical impedance spectroscopy (EIS) measurements were conducted using an HP 4194A Impedance/Gain-Phase Analyzer in the frequency range of 100 Hz to 15 MHz. Circular cut films were placed between two stainless steel flat electrodes in a parallel plate configuration to ensure uniform

contact and minimize interface resistance. The contact area was precisely defined as $0.5~\rm cm^2$ for conductivity calculations, and film thickness was measured using a micrometer. All impedance measurements were performed at room temperature (22 ± 2 °C) under ambient conditions (relative humidity ~50%) without active environmental control. The setup was allowed to thermally equilibrate before each measurement to ensure reproducibility.

3. RESULTS AND DISCUSSION

The wide-angle X-Ray diffraction patterns of the chitosan powder and chitosan films fabricated with different lactic acid concentrations are provided in **Figure 2** (a). Pure chitosan has an orthorhombic unit cell with a=8.129 Å, b=8.347 Å and c=10.311 Å [27]. Two broad characteristic peaks can be observed at $2\theta = 9.7^{\circ}$ and 20.2° . The peak at $2\theta = 9.7^{\circ}$ is assigned to (100) crystalline plane and associated with the hydrated crystals of low crystallinity described as crystal form I [28], [29]. The peak at $2\theta = 20.2^{\circ}$ is assigned to (200) plane which is described as crystal form II [29]. Chitosan films prepared with different lactic acid concentrations show similar XRD patterns. The peak at $2\theta = 9.7^{\circ}$ completely disappears for each lactic acid concentration. Intensity of the peak at $2\theta = 20.2^{\circ}$ decreases and becomes broader with lactic acid addition. Crystallinity index (CrI) of chitosan powder and chitosan films prepared with 2% wt. 4% wt. and 6% lactic acid solutions were calculated as 64%, 43%, 41% and 37%, respectively. These results indicate that lactic acid addition decreases crystallinity of chitosan. Similar XRD patterns were also observed in the literature for chitosan films fabricated with lactic acid [23], [30], [31].

FTIR spectrum of pure chitosan powder and chitosan films prepared with different lactic acid concentrations is provided in Figure 2 (b). Distinctive IR bands for pure chitosan powder are obtained at 1024 cm⁻¹ and 1058 cm⁻¹ (asymmetric and symmetric stretching of C-O (from ring)), 1150 cm⁻¹ (asymmetric vibrations of C-O (from glycosidic linkage)) [32], 1371 cm-1 (bending vibration of C-H from amide group) [33], 1560 cm⁻¹ (bending vibration of N-H from amide group) [33], 1645 cm⁻¹ (stretching vibration of C=O from amide I) [34], 2870 cm⁻¹ (symmetric and asymmetric stretching of C-H from ring CH₂OH and CH₃ groups) [35], 3350 cm⁻¹ (symmetric stretching of N-H), and broad band between 3000-3700 cm⁻¹ (stretching vibrations of OH groups) [36]. Distinctive IR bands of lactic acid were observed for the chitosan film samples fabricated with different lactic acid concentrations at 1122 cm⁻¹ and 1720 cm⁻¹. The peaks at 1122 cm⁻¹ and 1720 cm⁻¹ are assigned to C-O stretching of the secondary alcohol and C=O stretching of the carboxylic acid, respectively. The relative intensities of these peaks increase as the lactic acid concentration increases as expected. The position of the 1560 cm-1 peak assigned to the N-H bond shifted after the addition of lactic acid, as shown in Figure 2 (b). This peak was positioned at 1560 cm⁻¹ for chitosan powder and shifted to 1564 cm⁻¹, 1571 cm⁻¹ and 1573 cm⁻¹ when lactic acid concentration was 2 wt %, 4 wt % and 6 wt %, respectively. The peak shift has been also reported in the literature [31], [37], [38], [39]. It was attributed to interaction between amine groups in chitosan and carboxylic groups in lactic acid as the result of protonation.

TGA and DTG results of chitosan powder and chitosan films fabricated with different lactic acid concentrations between 35 °C and 550 °C are provided in **Figure 3 (a)** and **(b)**, respectively. Two stage decompositions were observed for chitosan powder. In the initial stage, a weight loss of 8% occurs between 35 °C and 150 °C. This weight loss was attributed to loss of absorbed and bounded water [40], [41]. A sharper weight loss corresponding to decomposition of chitosan backbone is observed between 250 °C and 450 °C with its maximum rate at 300 °C [42], [43]. The temperature for maximum decomposition rate for chitosan films decreases from 300 °C to 288 °C. This decrease can be explained by the transformation of chitosan from crystal to amorphous structure with the addition of lactic acid as observed in XRD patterns. Unlike chitosan powder, a third decomposition step having maximum rate at around 190 °C is observed for chitosan films prepared with different lactic acid concentrations. The step is attributed to the decomposition of lactic acid [44]. Intensity of the peak increases with increasing lactic acid concentration as observed in **Figure 3 (b)** as expected.

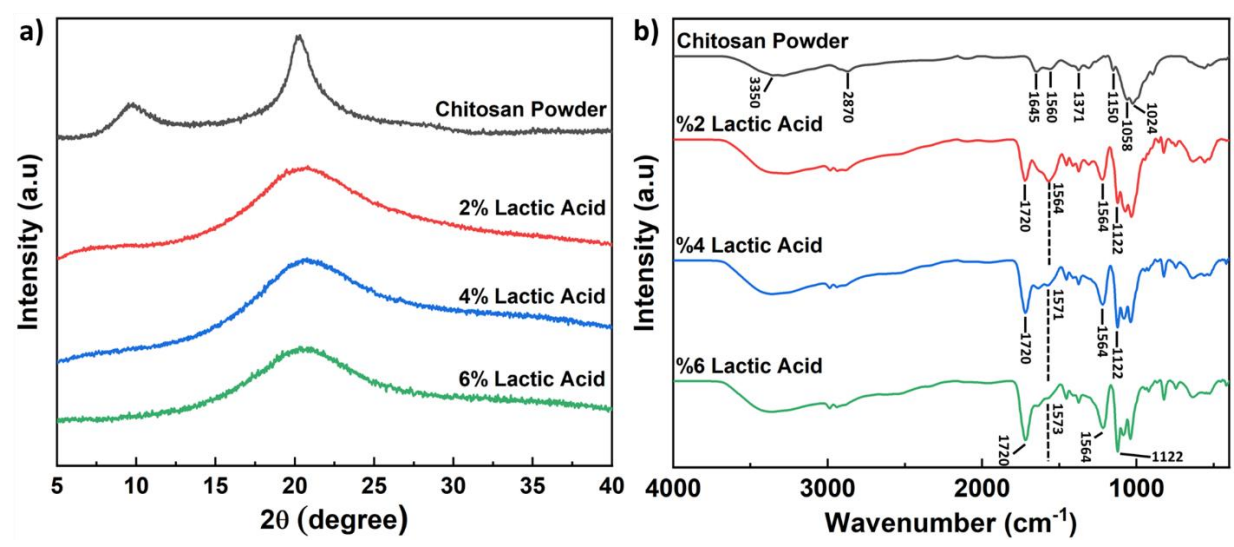


Figure 2: (a) X-ray diffraction patterns of chitosan powders and chitosan films prepared from acidic solutions with 2 wt%, 4 wt% and 6 wt% lactic acid concentrations. **(b)** FTIR spectra of chitosan powders and chitosan films prepared from acidic solutions with 2 wt%, 4 wt% and 6 wt% lactic acid concentrations.

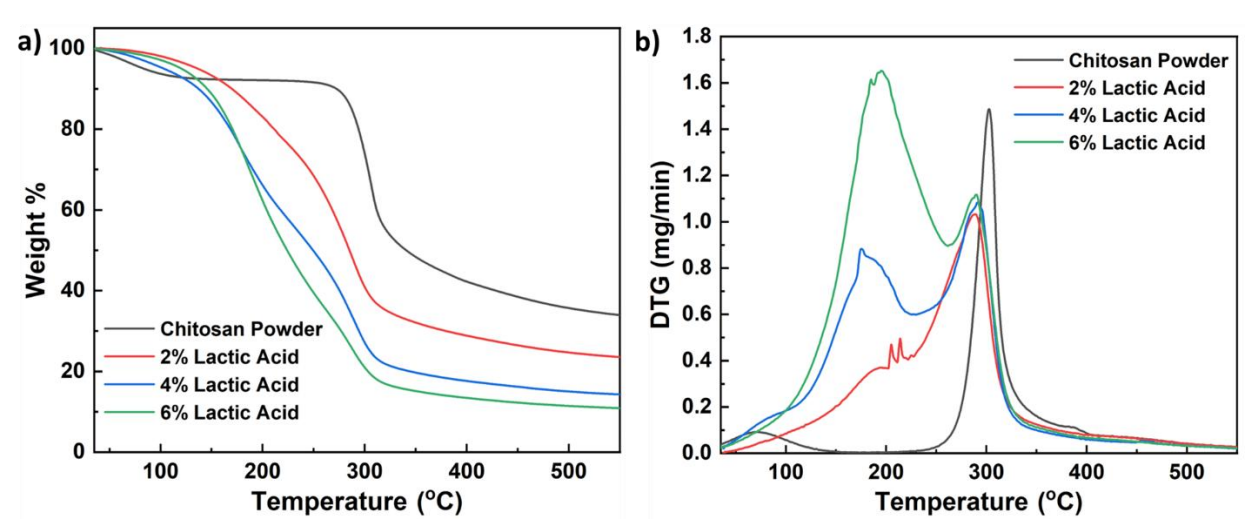


Figure 3: (a) TGA curves and **(b)** DTG curves (first derivative of weight % with respect to time) of chitosan powders and chitosan films prepared from different acidic solutions with 2%, 4% and 6% lactic acid concentrations.

Electrochemical characterizations of the chitosan films have an importance in understanding the effect of lactic acid concentration on the chemical structure. Complex impedance spectroscopy has been conducted to figure out structural properties of the chitosan films prepared with different acidic solutions. The results of impedance spectroscopies of chitosan films prepared with different lactic acid concentrations are provided in **Figure 4 (a)** and **(b)**. The impedance of chitosan films decreases upon increasing lactic acid concentration, as evidenced by the smaller semicircle observed from Nyguist plots. The end of the semi-circle at high frequencies is called bulk resistance, while the spikes at low frequencies correspond to the electrode polarization between chitosan films and metal contacts.

Ionically conductive behavior of chitosan films fabricated with different acidic solutions were previously reported [11]. The intrinsic ionic conduction of chitosan films was attributed to the free hydroxide ions formed as the result of the protonation reaction between amino groups and acids. Chitosan, in its native form and in the absence of redox-active dopants or conductive fillers, functions as a proton-conducting biopolymer with negligible intrinsic electronic conductivity. Therefore, the overall

conductivity observed in this study can be reasonably attributed to ionic transport mechanisms, although a minimal electronic contribution cannot be entirely excluded under ambient conditions. Ionic conductivities of chitosan films prepared from acidic solutions with 2%, 4% and 6% lactic acid concentrations are provided in **Figure 4** (c). The following equation was used to calculate ionic conductivities from the bulk resistance value obtained from Nyguist plots:

$$\delta = \frac{1}{R_h} \frac{d}{S}$$

where δ is ionic conductivity, R_b is bulk resistance, d is the thickness of the film S is the contact area. Ionic conductivities of chitosan films prepared from acidic solutions with 2 wt%, 4 wt% and 6 wt% lactic acid concentrations calculated as $4.8*10^{-7}$ S/cm, $5.6*10^{-5}$ S/cm and $2.6*10^{-4}$ S/cm, respectively. There are two possible reasons for the increase in ionic conductivity. Firstly, increasing the acid concentration enhances the protonation of chitosan's amino groups ($-NH_2$), leading to the formation of $-NH_3^+$ moieties through acid base interactions as show in the literature [45]. This protonation process increases the overall density of mobile charge carriers within the polymer matrix, as each protonated amine group contributes to the ionic transport mechanism via mobile protons. As previously discussed in the FTIR analysis (**Figure 2b**), the systematic shift of the N–H bending peak with increasing lactic acid concentration supports this interpretation by indicating progressive protonation. Consequently, higher acid concentrations result in an elevated concentration of free ions capable of participating in charge conduction. Moreover, the reduction in crystalline with increasing lactic acid concentration, as previously shown in the XRD analysis (**Figure 2a**), facilitates greater segmental mobility of the chitosan chains and charge carriers and contributes to the observed enhancement in ionic conductivity.

The areal capacitances of chitosan films produced from different lactic acid solutions were also investigated for use in applications like capacitive sensors, energy storage devices. Broadband areal capacitance measurements were conducted for this purpose as its results are provided in **Figure 4 (d)**. The areal capacitances are highly dependent on the lactic acid concentration. Polar ends of protonated chitosan chains and charge carriers are randomly oriented when there is no electric field applied on. On the other hand, the applied electric field aligns the polar ends and charge carriers through the field direction. At high frequency, polar ends and charge carriers cannot align rapid enough through the field direction. At low frequency, polar ends and charge carriers have enough time to travel macroscopic distance to align themselves through the field direction that causes an accumulation at the interface. This frequency dependent capacitance change by double layer formation near the electrode surface is often described as electrode polarization or Maxwell-Wagner-Silliars interfacial polarization. The areal capacitances at 100 Hz were measured as $0.026~\mu F/cm^2$, $3~\mu F/cm^2$ and $7.14~\mu F/cm^2$ for the chitosan films prepared with lactic acid concentration of 2%, 4% and 6%, respectively. This increase in areal capacitance with increasing lactic acid concentration was attributed to the same reasons discussed for the increase in ionic conductivity.

Table 1 provides a comparative overview of the ionic conductivity, areal capacitance, and application areas of gel electrolytes based on various biopolymers reported in the literature. While battery-oriented systems such as those using cellulose/LiPF₆ or chitosan/ZnSO₄ tend to deliver higher ionic conductivities (reaching up to 7.2×10^{-1} S/cm), many chitosan-based formulations demonstrate conductivity values in the 10^{-4} to 10^{-3} S/cm range. These are comparable to the performance observed in the present study. Specifically, the ionic conductivity of 2.6×10^{-4} S/cm achieved using lactic-acid-modified chitosan films aligns with values reported for similar systems, including chitosan/polyacrylamide (11×10^{-4} S/cm) and hydroxyethyl cellulose/glycerol (99×10^{-4} S/cm), which are employed in supercapacitors and pressure sensors. With respect to areal capacitance, the measured value of $7.14 \, \mu$ F/cm² is closely approaching or surpassing those of other biopolymer-based gels such as hydroxyethyl cellulose/glycerol ($12 \, \mu$ F/cm²) and P(HEMA)/cellulose ($3.2 \, \mu$ F/cm²). This performance highlights the suitability of the developed films for use in flexible dielectric interfaces and capacitive sensing technologies. A notable advantage of this work lies in its reliance on naturally derived, non-toxic

ingredients namely chitosan and lactic acid. In contrast to conventional gel electrolytes incorporating LiPF₆, ZnSO₄, or synthetic ionic liquids, the absence of hazardous species in this formulation enhances its compatibility with biomedical and environmentally sensitive applications, where non-toxicity and sustainability are essential.

Table 1. Ionic conductivity and areal capacitance values of various biopolymer gel electrolytes used in

electrochemical energy storage and sensing applications.

	,	Ionic	Areal		
Polymer	Electrolyte	Conductivity	Capacitance	Application	Ref
		S/cm ⁻¹	μF/cm²		
Cellulose	LiPF ₆	281*10-4		Li Based	[46]
				Batteries	
Hydroxypropyl methyl cellulose	LiPF6	38*10-4		Li Based	[47]
				Batteries	
Chitosan	ZnSO ₄	7200*10-4		Zn Based	[48]
Chitosan	Z113O4	7200 10 1		Batteries	
Silk Fibroin	Choline nitride	340*10-4		Mg Based	[49]
				Batteries	
Chitosan/Polyacrylamide	H ₂ PO ₄	H ₃ PO ₄ 11*10-4		Super	[50]
Chitosan/i oryaci ylannide	1131 04			Capacitors	
Na Alginate/ Polyacrylamide	Na ₂ SO ₄	50*10-4		Super	[51]
				Capacitors	
Hydroxyethyl				Capacitive	
cellulose/Glycerol	NaCl	99*10-4	12	Pressure	[52]
centilose/Glycerol				Sensors	
P(HEMA)/Cellulose	[EMIM][OTF]			Capacitive	
			3.2	Pressure	[53]
				Sensors	
Chitosan	Lactic Acid	2.6*10-4	7.14		This
					Work

The variation in lactic acid concentration significantly influenced the structural, thermal, and electrochemical properties of the chitosan films, offering valuable insights into their potential for practical applications. In particular, the electrochemical characteristics, namely ionic conductivity and areal capacitance exhibited a clear dependence on lactic acid content, indicating that these films are promising candidates for use in electrochemical devices. These findings contribute to a deeper understanding of chitosan-based systems and establish a foundation for future efforts to optimize their performance for targeted applications. It is important to note that the ionic conductivity of chitosan films is strongly affected by ambient humidity, as water molecules act both as plasticizers and ion transport facilitators within the polymer matrix. Previous studies on chitosan-based sensors have reported conductance variations of up to four orders of magnitude as relative humidity increased from 10 % to 90 % RH, highlighting the substantial role of environmental moisture in modulating ionic conductivity [54]. In our study, impedance measurements were carried out under ambient laboratory conditions (~50 % RH); however, systematic humidity control was not implemented. Future investigations should explore the impact of controlled humidity environments to better elucidate ion transport mechanisms and to assess the suitability of these films in variable ambient conditions particularly for wearable or implantable devices. Further research should also examine the long-term stability, mechanical robustness, and biocompatibility of these films to fully realize their potential in applications such as biomedical devices, electrochemical sensors, and energy storage systems.

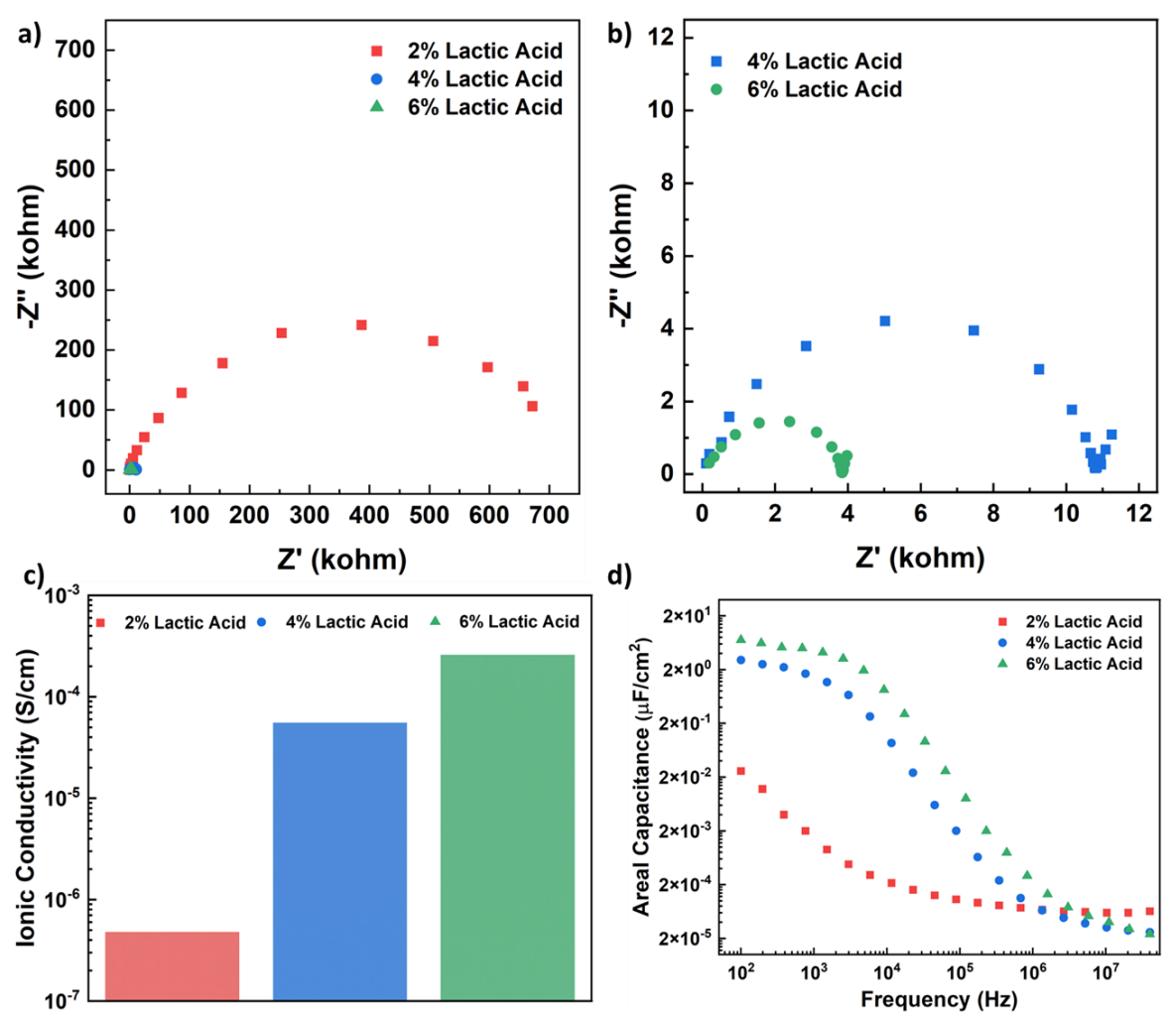


Figure 4: (a) Nyquist plots of chitosan films prepared from different acidic solutions with 2%, 4% and 6% lactic acid concentrations and **(b)** Nyquist plot of the chitosan films prepared with 4% and 6% lactic acid solutions. **(c)** Ionic conductivity measurements and **(d)** Areal capacitance measurements of chitosan films prepared with 2% wt. 4% wt. and 6% lactic acid solutions.

4. CONCLUSIONS

This research demonstrated that varying lactic acid concentrations significantly influence the structural, thermal, and electrochemical properties of chitosan films. The increase in lactic acid concentration reduced the crystallinity of the chitosan films, as confirmed by X-ray diffraction analysis. FTIR results indicated stronger interactions between chitosan and lactic acid with increasing acid concentration, leading to shifts in characteristic IR bands of N-H bond positioned around 1560 cm⁻¹. Thermogravimetric analysis revealed that higher concentrations of lactic acid lowered the decomposition temperature of the chitosan films, indicating decreased thermal stability. The maximum decomposition rate of pristine chitosan powder occurred at approximately 300 °C, whereas chitosan films processed with lactic acid solutions exhibited a decreased peak at 288 °C. Increasing lactic acid concentration did not result in a significant shift in the peak decomposition temperature. Electrochemical characterization revealed a pronounced enhancement in both ionic conductivity and areal capacitance of chitosan films with increasing lactic acid concentration in the precursor solution. The ionic conductivity values of the films prepared with 2 wt%, 4 wt%, and 6 wt% lactic acid were determined to be 4.8 × 10⁻⁷ S/cm, 5.6 × 10⁻⁵ S/cm, and 2.6 × 10⁻⁴ S/cm, respectively. Correspondingly, the

areal capacitances measured at 100 Hz were $0.026\,\mu\text{F/cm}^2$, $3.00\,\mu\text{F/cm}^2$, and $7.14\,\mu\text{F/cm}^2$ for films fabricated with 2%, 4%, and 6% lactic acid, respectively. These results highlight the efficacy of lactic acid as a green processing agent, enabling the fabrication of chitosan-based films with tunable electrochemical performance. Such films exhibit significant potential for integration into energy storage platforms, capacitive sensing technologies, wearable electronics, and implantable biomedical systems.

Declaration of Ethical Standards

The authors declare that the study complies with all applicable laws and regulations and meets ethical standards.

Declaration of Competing Interest

The authors declare that there is no conflict of interest.

Acknowledgements

Melih Ogeday Cicek is gratefully acknowledged for his help with electrochemical measurements and consequent interpretation thereof.

Data Availability

The data that support the findings of this study are available from the corresponding author upon reasonable request.

REFERENCES

- [1] J. Lv, X. Lv, M. Ma, D.-H. Oh, Z. Jiang, and X. Fu, "Chitin and chitin-based biomaterials: A review of advances in processing and food applications," *Carbohydr Polym*, vol. 299, p. 120142, Jan. 2023, doi: 10.1016/j.carbpol.2022.120142.
- [2] J. Wang and S. Zhuang, "Chitosan-based materials: Preparation, modification and application," *J Clean Prod*, vol. 355, p. 131825, Jun. 2022, doi: 10.1016/j.jclepro.2022.131825.
- [3] S. Peers, A. Montembault, and C. Ladavière, "Chitosan hydrogels for sustained drug delivery," *Journal of Controlled Release*, vol. 326, pp. 150–163, Oct. 2020, doi: 10.1016/j.jconrel.2020.06.012.
- [4] U. Garg, S. Chauhan, U. Nagaich, and N. Jain, "Current Advances in Chitosan Nanoparticles Based Drug Delivery and Targeting," *Adv Pharm Bull*, vol. 9, no. 2, pp. 195–204, Jun. 2019, doi: 10.15171/apb.2019.023.
- [5] T. Dai, M. Tanaka, Y.-Y. Huang, and M. R. Hamblin, "Chitosan preparations for wounds and burns: antimicrobial and wound-healing effects," *Expert Rev Anti Infect Ther*, vol. 9, no. 7, pp. 857–879, Jul. 2011, doi: 10.1586/eri.11.59.
- [6] H. Wang, J. Qian, and F. Ding, "Emerging Chitosan-Based Films for Food Packaging Applications," *J Agric Food Chem*, vol. 66, no. 2, pp. 395–413, Jan. 2018, doi: 10.1021/acs.jafc.7b04528.
- [7] F. Demir, G. Gökşen, And D. Demir Karakuş, "Effect Of Orange Peel Essential Oil On The Properties Of Chitosan: Gelatin Casted Films Prepared For Active Packaging," *Konya Journal of Engineering Sciences*, Vol. 11, no. 3 pp. 668–677, May 2023, doi: 10.36306/konjes.1225056.
- [8] A. Kazan And F. Demirci, "Olive Leaf Extract Incorporated Chitosan Films For Active Food Packaging," *Konya Journal Of Engineering Sciences*, Vol. 11, no. 4, Pp. 1061–1072, Dec. 2023, Doi: 10.36306/Konjes.1310528.
- [9] K. Xing, X. Zhu, X. Peng, and S. Qin, "Chitosan antimicrobial and eliciting properties for pest control in agriculture: a review," *Agron Sustain Dev*, vol. 35, no. 2, pp. 569–588, Apr. 2015, doi: 10.1007/s13593-014-0252-3.

- [10] S. Wu, S. Wu, X. Zhang, T. Feng, and L. Wu, "Chitosan-Based Hydrogels for Bioelectronic Sensing: Recent Advances and Applications in Biomedicine and Food Safety," *Biosensors (Basel)*, vol. 13, no. 1, p. 93, Jan. 2023, doi: 10.3390/bios13010093.
- [11] B. Ronnasi, S. P. McKillop, M. Ourabi, M. Perry, H. A. Sharp, and B. H. Lessard, "Chitosan-Based Electronics: The Importance of Acid Strength and Plasticizing Additives on Device Performance," *ACS Appl Mater Interfaces*, Nov. 2024, doi: 10.1021/acsami.4c10508.
- [12] C. Hu, L. Wang, S. Liu, X. Sheng, and L. Yin, "Recent Development of Implantable Chemical Sensors Utilizing Flexible and Biodegradable Materials for Biomedical Applications," *ACS Nano*, vol. 18, no. 5, pp. 3969–3995, Feb. 2024, doi: 10.1021/acsnano.3c11832.
- [13] J. Zou, K. Zhang, and Q. Zhang, "Giant Humidity Response Using a Chitosan-Based Protonic Conductive Sensor," *IEEE Sens J*, vol. 16, no. 24, pp. 8884–8889, Dec. 2016, doi: 10.1109/JSEN.2016.2616484.
- [14] M. Zhang, A. Smith, and W. Gorski, "Carbon Nanotube–Chitosan System for Electrochemical Sensing Based on Dehydrogenase Enzymes," *Anal Chem*, vol. 76, no. 17, pp. 5045–5050, Sep. 2004, doi: 10.1021/ac049519u.
- [15] S. Wu *et al.*, "Recent Advances in Chitosan-Based Hydrogels for Flexible Wearable Sensors," Jan. 01, 2023, *Multidisciplinary Digital Publishing Institute (MDPI)*. doi: 10.3390/chemosensors11010039.
- [16] S. (Gabriel) Kou, L. Peters, and M. Mucalo, "Chitosan: A review of molecular structure, bioactivities and interactions with the human body and micro-organisms," *Carbohydr Polym*, vol. 282, p. 119132, Apr. 2022, doi: 10.1016/j.carbpol.2022.119132.
- [17] C. Qiao, X. Ma, X. Wang, and L. Liu, "Structure and properties of chitosan films: Effect of the type of solvent acid," *LWT*, vol. 135, p. 109984, Jan. 2021, doi: 10.1016/j.lwt.2020.109984.
- [18] C. Caner, P. J. Vergano, and J. L. Wiles, "Chitosan Film Mechanical and Permeation Properties as Affected by Acid, Plasticizer, and Storage," *J Food Sci*, vol. 63, no. 6, pp. 1049–1053, Nov. 1998, doi: 10.1111/j.1365-2621.1998.tb15852.x.
- [19] W. Zhang *et al.*, "The role of organic acid structures in changes of physicochemical and antioxidant properties of crosslinked chitosan films," *Food Packag Shelf Life*, vol. 31, p. 100792, Mar. 2022, doi: 10.1016/j.fpsl.2021.100792.
- [20] M. G. Goñi, B. Tomadoni, S. I. Roura, and M. del R. Moreira, "Lactic acid as potential substitute of acetic acid for dissolution of chitosan: preharvest application to Butterhead lettuce," J Food Sci Technol, vol. 54, no. 3, pp. 620–626, Mar. 2017, doi: 10.1007/s13197-016-2484-5.
- [21] K. M. Kim, J. H. Son, S.-K. Kim, C. L. Weller, and M. A. Hanna, "Properties of Chitosan Films as a Function of pH and Solvent Type," *J Food Sci*, vol. 71, no. 3, pp. E119–E124, Jun. 2006, doi: 10.1111/j.1365-2621.2006.tb15624.x.
- [22] X. Qu, A. Wirsén, and A.-C. Albertsson, "Effect of lactic/glycolic acid side chains on the thermal degradation kinetics of chitosan derivatives," *Polymer (Guildf)*, vol. 41, no. 13, pp. 4841–4847, Jun. 2000, doi: 10.1016/S0032-3861(99)00704-1.
- [23] X. Dou, Q. Li, Q. Wu, L. Duan, S. Zhou, and Y. Zhang, "Effects of lactic acid and mixed acid aqueous solutions on the preparation, structure and properties of thermoplastic chitosan," *Eur Polym J*, vol. 134, p. 109850, Jul. 2020, doi: 10.1016/j.eurpolymj.2020.109850.
- [24] D. G. Mackanic *et al.*, "Decoupling of mechanical properties and ionic conductivity in supramolecular lithium ion conductors," *Nat Commun*, vol. 10, no. 1, p. 5384, Nov. 2019, doi: 10.1038/s41467-019-13362-4.
- [25] J. Chattopadhyay, T. S. Pathak, and D. M. F. Santos, "Applications of Polymer Electrolytes in Lithium-Ion Batteries: A Review," *Polymers (Basel)*, vol. 15, no. 19, p. 3907, Sep. 2023, doi: 10.3390/polym15193907.
- [26] L. Segal, J. J. Creely, A. E. Martin, and C. M. Conrad, "An Empirical Method for Estimating the Degree of Crystallinity of Native Cellulose Using the X-Ray Diffractometer," *Textile Research Journal*, vol. 29, no. 10, pp. 786–794, Oct. 1959, doi: 10.1177/004051755902901003.

[27] P. Naito, Y. Ogawa, D. Sawada, Y. Nishiyama, T. Iwata, and M. Wada, "X-ray crystal structure of anhydrous chitosan at atomic resolution," *Biopolymers*, vol. 105, no. 7, pp. 361–368, Jul. 2016, doi: 10.1002/bip.22818.

- [28] K. Ogawa and T. Yui, "Effect of Explosion on the Crystalline Polymorphism of Chitin and Chitosan," *Biosci Biotechnol Biochem*, vol. 58, no. 5, pp. 968–969, Jan. 1994, doi: 10.1271/bbb.58.968.
- [29] R. J. Samuels, "Solid state characterization of the structure of chitosan films," *Journal of Polymer Science: Polymer Physics Edition*, vol. 19, no. 7, pp. 1081–1105, Jul. 1981, doi: 10.1002/pol.1981.180190706.
- [30] I. Kondratowicz *et al.*, "Impact of Lactic Acid and Genipin Concentration on Physicochemical and Mechanical Properties of Chitosan Membranes," *J Polym Environ*, vol. 31, no. 3, pp. 1221–1231, Mar. 2023, doi: 10.1007/s10924-022-02691-z.
- [31] X. Qu, A. Wirson, and A.-C. Albertsson, "Synthesis and characterization of pH-sensitive hydrogels based on chitosan and D,L-lactic acid," *J Appl Polym Sci*, vol. 74, no. 13, pp. 3193–3202, Dec. 1999, doi: 10.1002/(SICI)1097-4628(19991220)74:13<3193::AID-APP23>3.0.CO;2-V.
- [32] C. Paluszkiewicz, E. Stodolak, M. Hasik, and M. Blazewicz, "FT-IR study of montmorillonite—chitosan nanocomposite materials," *Spectrochim Acta A Mol Biomol Spectrosc*, vol. 79, no. 4, pp. 784–788, Aug. 2011, doi: 10.1016/j.saa.2010.08.053.
- [33] A. Pawlak and M. Mucha, "Thermogravimetric and FTIR studies of chitosan blends," *Thermochim Acta*, vol. 396, no. 1–2, pp. 153–166, Feb. 2003, doi: 10.1016/S0040-6031(02)00523-3.
- [34] M. Darder, M. Colilla, and E. Ruiz-Hitzky, "Chitosan–clay nanocomposites: application as electrochemical sensors," *Appl Clay Sci*, vol. 28, no. 1–4, pp. 199–208, Jan. 2005, doi: 10.1016/j.clay.2004.02.009.
- [35] M. L. Duarte, M. C. Ferreira, M. R. Marvão, and J. Rocha, "An optimised method to determine the degree of acetylation of chitin and chitosan by FTIR spectroscopy," *Int J Biol Macromol*, vol. 31, no. 1–3, pp. 1–8, Dec. 2002, doi: 10.1016/S0141-8130(02)00039-9.
- [36] Y. Shigemasa, H. Matsuura, H. Sashiwa, and H. Saimoto, "Evaluation of different absorbance ratios from infrared spectroscopy for analyzing the degree of deacetylation in chitin," *Int J Biol Macromol*, vol. 18, no. 3, pp. 237–242, Apr. 1996, doi: 10.1016/0141-8130(95)01079-3.
- [37] C. Qiao, X. Ma, X. Wang, and L. Liu, "Structure and properties of chitosan films: Effect of the type of solvent acid," *LWT*, vol. 135, p. 109984, Jan. 2021, doi: 10.1016/j.lwt.2020.109984.
- [38] K. M. Kim, J. H. Son, S.-K. Kim, C. L. Weller, and M. A. Hanna, "Properties of Chitosan Films as a Function of pH and Solvent Type," *J Food Sci*, vol. 71, no. 3, pp. E119–E124, Jun. 2006, doi: 10.1111/j.1365-2621.2006.tb15624.x.
- [39] I. Kondratowicz *et al.*, "Impact of Lactic Acid and Genipin Concentration on Physicochemical and Mechanical Properties of Chitosan Membranes," *J Polym Environ*, vol. 31, no. 3, pp. 1221–1231, Mar. 2023, doi: 10.1007/s10924-022-02691-z.
- [40] K. Lewandowska, "Miscibility and thermal stability of poly(vinyl alcohol)/chitosan mixtures," *Thermochim Acta*, vol. 493, no. 1–2, pp. 42–48, Sep. 2009, doi: 10.1016/j.tca.2009.04.003.
- [41] J. M. F. Pavoni, C. L. Luchese, and I. C. Tessaro, "Impact of acid type for chitosan dissolution on the characteristics and biodegradability of cornstarch/chitosan based films," *Int J Biol Macromol*, vol. 138, pp. 693–703, Oct. 2019, doi: 10.1016/j.ijbiomac.2019.07.089.
- [42] I. Quijadagarrido, V. Iglesiasgonzalez, J. Mazonarechederra, And J. Barralesrienda, "The role played by the interactions of small molecules with chitosan and their transition temperatures. Glass-forming liquids: 1,2,3-Propantriol (glycerol)," *Carbohydr Polym*, vol. 68, no. 1, pp. 173–186, Mar. 2007, doi: 10.1016/j.carbpol.2006.07.025.
- [43] J. Khouri, A. Penlidis, and C. Moresoli, "Heterogeneous method of chitosan film preparation: Effect of multifunctional acid on film properties," *J Appl Polym Sci*, vol. 137, no. 18, May 2020, doi: 10.1002/app.48648.

- [44] W. Tang *et al.*, "Facile pyrolysis synthesis of ionic liquid capped carbon dots and subsequent application as the water-based lubricant additives," *J Mater Sci*, vol. 54, no. 2, pp. 1171–1183, Jan. 2019, doi: 10.1007/s10853-018-2877-0.
- [45] M. L. Amorim *et al.*, "Physicochemical Aspects of Chitosan Dispersibility in Acidic Aqueous Media: Effects of the Food Acid Counter-Anion," *Food Biophys*, vol. 11, no. 4, pp. 388–399, Dec. 2016, doi: 10.1007/s11483-016-9453-4.
- [46] J. Wan, J. Zhang, J. Yu, and J. Zhang, "Cellulose Aerogel Membranes with a Tunable Nanoporous Network as a Matrix of Gel Polymer Electrolytes for Safer Lithium-Ion Batteries," *ACS Appl Mater Interfaces*, vol. 9, no. 29, pp. 24591–24599, Jul. 2017, doi: 10.1021/acsami.7b06271.
- [47] Y. Ran, Z. Yin, Z. Ding, H. Guo, and J. Yang, "A polymer electrolyte based on poly(vinylidene fluoride-hexafluoropylene)/hydroxypropyl methyl cellulose blending for lithium-ion battery," *Ionics* (*Kiel*), vol. 19, no. 5, pp. 757–762, May 2013, doi: 10.1007/s11581-012-0808-7.
- [48] M. Wu *et al.*, "A sustainable chitosan-zinc electrolyte for high-rate zinc-metal batteries," *Matter*, vol. 5, no. 10, pp. 3402–3416, Oct. 2022, doi: 10.1016/j.matt.2022.07.015.
- [49] X. Jia *et al.*, "A Biodegradable Thin-Film Magnesium Primary Battery Using Silk Fibroin–Ionic Liquid Polymer Electrolyte," *ACS Energy Lett*, vol. 2, no. 4, pp. 831–836, Apr. 2017, doi: 10.1021/acsenergylett.7b00012.
- [50] J. Xu, R. Jin, X. Ren, and G. Gao, "A wide temperature-tolerant hydrogel electrolyte mediated by phosphoric acid towards flexible supercapacitors," *Chemical Engineering Journal*, vol. 413, p. 127446, Jun. 2021, doi: 10.1016/j.cej.2020.127446.
- [51] J. Zeng, L. Dong, W. Sha, L. Wei, and X. Guo, "Highly stretchable, compressible and arbitrarily deformable all-hydrogel soft supercapacitors," *Chemical Engineering Journal*, vol. 383, p. 123098, Mar. 2020, doi: 10.1016/j.cej.2019.123098.
- [52] M. O. Cicek *et al.*, "Ultra-Sensitive Bio-Polymer Iontronic Sensors for Object Recognition from Tactile Feedback," *Adv Mater Technol*, vol. 8, no. 16, Aug. 2023, doi: 10.1002/admt.202300322.
- [53] S. Li, J. Chu, B. Li, Y. Chang, and T. Pan, "Handwriting Iontronic Pressure Sensing Origami," *ACS Appl Mater Interfaces*, vol. 11, no. 49, pp. 46157–46164, Dec. 2019, doi: 10.1021/acsami.9b16780.
- [54] J. Zou, K. Zhang, and Q. Zhang, "Giant Humidity Response Using a Chitosan-Based Protonic Conductive Sensor," *IEEE Sens J*, vol. 16, no. 24, pp. 8884–8889, Dec. 2016, doi: 10.1109/JSEN.2016.2616484.